Partitioning of rare earth elements between phosphate-rich carbonatite melts and mantle peridotites

Article *in* Mineralogy and Petrology · March 1993

DOI: 10.1007/BF01162922

CITATIONS
14

READS
39

4 authors, including:

I. D. Ryabchikov
Russian Academy of Sciences
153 PUBLICATIONS **2,089** CITATIONS
SEE PROFILE

Senin Valery
Russian Academy of Sciences
72 PUBLICATIONS **275** CITATIONS
SEE PROFILE

Mineralogy and Petrology (1993) 49: 1–12

Mineralogy and Petrology

Partitioning of Rare Earth Elements Between Phosphate-rich Carbonatite Melts and Mantle Peridotites

I. D. Ryabchikov[1], G. P. Orlova[1], V. G. Senin[2], and N. V. Trubkin[1]

[1] Institute for Geology of Ore Deposits, Petrography, Mineralogy and Geochemistry, Academy of Sciences, Moscow, Russia
[2] V. I. Vernadsky Institute of Geochemistry and Analytical Chemistry, Academy of Sciences, Moscow, Russia

With 2 Figures

Received June 14, 1991;
accepted December 28, 1992

Summary

Near solidus equilibria in the system mantle peridotite-carbonate-phosphate doped with Ce and Yb have been studied at 20 kbar and 950 °C. Carbonatitic melts in this system may be quenched into homogeneous glasses. Such melts intensely extract REE from rock-forming mantle minerals, and their migration may cause processes of mantle metasomatism.

Zusammenfassung

Verteilung von Seltenen Erden zwischen phosphatreichen karbonatitischen Schmelzen und Mantel-Peridotiten

Gleichgewichte nahe dem Solidus im System Mantel-Peridotit–Karbonat–Phosphat, das mit Ce und Yb dotiert wurde, wurden bei 20 kbar und 950 °C untersucht. Karbonatitische Schmelzen in diesem System können zu homogenen Gläsern abgeschreckt werden. Solche Schmelzen extrahieren SEE aus gesteinsbildenden Mantelmineralen und ihre Migration könnte für Vorgänge der Mantel-Metasomatose verantwortlich sein.

Introduction

Carbonate melts which may coexist at high pressures with mantle peridotites are attracting increasing interest. This is related to their possible role as agents of mantle metasomatism, and it has also been suggested that certain carbonatites are the result

of this juvenile melt reaching the surface (*Bailey*, 1989). Recent advances in the field of physico-chemical petrology related to the genesis of crustal and primary carbonatitic melts as well as the integrated model for the generation of crustal carbonatites are given by *Wyllie* et al. (1990).

Due to the very low average abundances of volatile components in mantle material carbonate melts can only arise by very small degrees of partial melting, because at temperatures substantially above the solidus silicate components predominate in the liquid phase. Under near-solidus conditions it is expected that many incompatible components will be drastically transferred into the interstitial liquid. Phosphorus may play a particularly important role in this low degree melting process, and because its abundance in the mantle is comparable with that of CO_2 the possibility exists that very phosphate-rich carbonate melts are produced under some PT-conditions. Partial melting of carbonate- and phosphate-bearing peridotites was previously studied at 30 kbar (*Ryabchikov* et al., 1991); this paper extends this latter study down to 20 kbar. Additionally we have doped our experimental charges with some REE's in order to investigate inter-phase distribution of these elements and to elucidate the factors controlling their behaviour in the processes of mantle metasomatism involving carbonate-rich melts (*Green* and *Wallace*, 1988; *Ryabchikov* et al., 1993).

Starting Materials

Starting materials were prepared as mixtures by grinding under acetone natural and syntetic minerals with added Na_2CO_3, CeO_2 and Yb_2O_3 reagents. The grain size in these powders was less than 0.02–0.03 mm. Mineral compositions are given in Table 1, and compositions of starting mixtures are shown in Table 2. Starting mixtures for experiments 3 and 4 contained about 1 wt% of both REE oxides. This is of course much higher than found in natural peridotites, but these high concentrations make it possible to use the electron probe microanalyser to measure the REE concentrations in the coexisting phases. We have chosen Ce and Yb as the representatives of light and heavy REE respectively, because the L_2-lines in their X-ray spectra do not overlap.

Experimental Method

Approximately 20 mg of starting material was placed into $Ag_{40}Pd_{60}$ capsules with 3 mm external diameter and length not more than 5 mm. Capsules were sealed by welding in a DC arc. Experiments at 950 °C and 20 kbar were conducted in the piston-cylinder high-pressure apparatus by the conventional quenching method described in detail by *Ryabchikov* et al. (1989). Talc-pyrex cells have been employed for experimental runs, and oxygen fugacities were not controlled. Run duration for anhydrous starting materials was 48 hours, while for mixtures with 0.4 wt% H_2O it was 34 hours.

Pressure calibration was performed by the bracketing of albite = jadeite + nepheline equilibrium at 800 °C, and it was found that approximately +10% correction for the "hot piston in" technique employed in the present work should be introduced. Pressure of our experiments is believed to be in the range of 20 ± 1 kbar.

No attempts were made to reach equilibrium from various directions, and, therefore, the results of the experiments reported are considered to be preliminary. However, crystals of clinopyroxene and apatite are quite homogeneous, and their composition is different from

Table 1. *Chemical compositions (wt%) of minerals used for starting mixes*

Mineral	Oxides											
	SiO_2	TiO_2	Al_2O_3	Cr_2O_3	FeO	MgO	CaO	Na_2O	P_2O_5	Ce_2O_3	MnO	Total
Dolomite	—	—	—	—	3.3	17.5	29.0	—	—	—	—	49.8
Hydro-xyapatite	—	—	—	—	—	—	55.82	—	42.39	—	—	98.21
Apatite	0.62	—	0.02	—	0.03	n.d.	54.80	0.15	39.79	0.94	—	96.35
Garnet	39.79	1.17	20.73	0.35	13.28	17.28	4.84	0.11	—	—	0.40	97.95
Clinopyroxene	52.30	0.65	7.09	0.67	2.90	14.94	19.40	2.09	—	—	0.09	100.13
Enstatite	58.01	0.03	0.79	0.16	5.24	35.12	0.22	0.04	—	—	0.09	99.70
Olivine	40.62	—	—	—	10.15	47.88	0.06	—	—	—	0.12	98.83

Dolomite from Kirghistan contains 49.8% CO_2 (calculation)
Hydroxyapatite contains according to stoichiometry 1.79% H_2O. This material was synthesized by M. Korzhinsky, Institute of Experimental Mineralogy AS USSR.
Apatite from the Khibina massif.
Garnet (sample FRB-335, collection of *F. R. Boyd*), discrete nodule, Angola.
Clinopyroxene from spinel peridotite nodule, Mongolia (collection of *V. I. Kovalenko*).
Enstatite (sample 351) from the nodule of garnet peridotite.
Olivine (sample 40/3), megacryst from *W. Eifel*, Germany; also contains 0.32% NiO.

Table 2. *Results of experiments with peridotite–carbonate–phosphate compositions at 950 °C, 20 kbar*

Run number	Duration, hours	Components in starting mixture (wt%)*	Phases in run products
2	48	5.1 Ga + 6.2 Cpx + 15.4 En 22.2 Ol + 21.7 Dol + 25.3 Ap + 4.1 Na_2CO_3	Ol + Cpx + Ap + intergranular glass
3	34	5.8 Ga + 6.6 Cpx + 15.5 En + 22.7 Ol + 20.9 Dol + 22.4 OH–Ap + 4.0 Na_2CO_3 + 1.1 CeO_2 + 0.9 Yb_2O_3	Ol + Cpx + Ap + patches of glass, visible under binocular microscope
4	34	5.1 Ga + 7.1 Cpx + 15.3 En + 22.2 Ol + 21.1 Dol + 22.6 OH–Ap + 4.1 Na_2CO_3 + 1.4 CeO_2 + 0.9 Yb_2O_3	Ol + Cpx + Ap + separate mass of glass with rare grains of Cr–Al spinel and olivine

* The compositions of minerals are given in Table 1

phases in starting material. All the garnet and practically all the othopyroxene added to the initial mix are consumed during experiments by interaction with the carbonate-rich melt. All this suggests that equilibrium was closely approached in our experiments. Considering low values of diffusion coefficients for crystalline phases, the most likely mechanism for attaining equilibrium is dissolution of old and precipitation of new crystals, rather than a diffusion in the solid state. *Brennan* and *Watson* (1991) demonstrated that equilibrium between silicate crystals and carbonate melts is attained within ca. 48 hours, which is comparable with our run durations.

Quenched run products were examined under the microscope, and later with the electron probe micro analyser and electron microscope (both SEM and TEM). A CAMEBAX MICROBEAM electron microprobe has been used in the present work with the accelerating voltage of 15 kV and a sample current of $3 \cdot 10^{-8}$ amps. Analyzed (by wet chemistry) apatite, andradite, albite, MgO, and $MnTiO_3$ samples together with synthetic $NaYb_3Si_{12}O_{36}$ and CeP_5O_{14} were used as the reference materials.

Experimental results

Run conditions and inferred equilibrium phase assemblages are given in Table 2. All run products contain olivine, Ca-rich clinopyroxene and apatite as equilibrium crystalline phases. Small grains of orthopyroxene surrounded by clinopyroxene rims are extremely rare and most likely represent relict minerals from the starting mixes which failed to react with the melt. Carbonate-phosphate-rich liquids quenched into glasses in all the run products; those glasses are sometimes slightly devitrified near the contacts with primary solid phases. A comparison of run products from experiments 3 and 4 with those from experiment 2 shows that, in the presence of 0.4 wt% H_2O and larger amounts of Ce and Yb (exp. 3 and 4), the solidus is noticeably lowered, i.e. there is a larger proportion of glass in 3 and 4 compared with exp. 2. Products of 2 (anhydrous, lower REE content) contained only thin films of

intergranular glass (Fig. 1a), while pools of glass were quite obvious in the products of 3, and in 4 solid minerals had settled at the bottom of container producing a large pool of clear glass in the upper part. Melt formed during exp. 2 (low REE, no H_2O) contained only small concentrations of SiO_2 while glasses from experiments 3 and 4 are much richer in silicates, implying that they were formed at temperatures significantly exceeding the solidus. Similar glasses with a composition close to the eutectic in the system $CaCO_3$–$Ca(OH)_2$–CaF_2–$BaSO_4$–$La(OH)_3$ at 1 kbar and 700–500 °C were described by *Jones* and *Wyllie* (1983).

Run 2 contains small patches of glass; these were analyzed by electron microprobe with the beam 2 microns in diameter, and a certain error due to the influence of surrounding crystals cannot be excluded. Large pools of quenched liquid in experiments 3 and 4 were analyzed with good reproducibility by scanning the electron beam through 25 × 25 microns area. The compositions of glasses are given in Table 2, the totals are considerably below 100% due to the presence in the glasses of volatiles (CO_2 and possibly H_2O). The presence of CO_2 was qualitatively established by the treatment of glass with diluted HCl, which revealed the appearance of abundant gas.

A substantial solubility of phosphorus in melts equilibrated with apatite has been established. The saturation of apatite in the absence of water at 20 kbar and 950 °C is reached at ca. 18 wt% P_2O_5 (experiment 2), but phosphorus concentration drops to 13–14 wt.% for more silica-rich melts, produced in the presence of water and with larger contents of REE.

Table 2 also shows the results of probe-analyses of apatites, olivines and clinopyroxenes coexisting with a melt under given experimental conditions. It permits the calculation of partition coefficients for various components including REE. (Table 3). The highest concentrations of rare earths were found in apatites. The process of isomorphous substitution in the structure of this mineral is likely to comply with the following schemes (*Ronsbo*, 1989; *Watson* and *Green*, 1981):

$$Ca^{2+} + P^{5+} = REE^{3+} + Si^{4+}$$

$$2Ca^{2+} = Na^{1+} + REE^{3+}$$

These reactions are supported by the fact that with increasing concentrations of Na, Si, Ce and Yb in the apatites Ca and P contents decrease distinctly.

The Ce and Yb contents of clinopyroxenes and particularly of olivines are rather low, and this results in a low precision for these analyses. Measured values may also be affected by the influence of intergranular carbonate-phosphate matrix which is strongly enriched in REE.

Considering, however, that these equilibria depend upon temperature, pressure, oxygen fugacity and composition of the liquid phase, the results summarized in Table 3 are, in general, comparable to previously published data on REE partition coefficients in experimental systems and natural rocks (*Agaphonov* and *Erkushev*, 1988; *Irving* and *Frey*, 1984; *Wass* et al., 1980; *Wendlandt* and *Harison* 1979). For example, our experimental values of $K_{Ce}^{Ap/Cpx}$ range from 10.6 to 14.3 and $K_{Yb}^{Ap/Cpx}$ range from 2.6 to 3.3. These are only slightly lower than the values established for apatite-bearing xenoliths in basaltic rocks of Western Australia (22 for Ce and 5 for Yb). These last two values were interpreted as the result of crystallisation of carbonate-kimberlite magma (*Wass* et al., 1980). Our measurements show that the Ce partition coefficient is 2–3 times lower and the Yb partition coefficient is 2 times lower for the apatite + near-solidus melt pair in the peridotite-phosphate-carbonate system as compared with the same mineral, equilibrated with basanitic melt (*Watson* and *Green*, 1981). Our data for clinopyroxene/liquid partition coefficients are also very similar to apatite-free peridotite-carbonate system (0.16 for Ce and 0.3 for Yb—*Brenan* and *Watson*, 1991). It could be argued that data from our experimental charges, because of their much higher concentrations of REE's, are not applicable to natural rock systems, but data by *Green* et al. (1989) have shown that this higher level of REE's has no significant effect on distribution

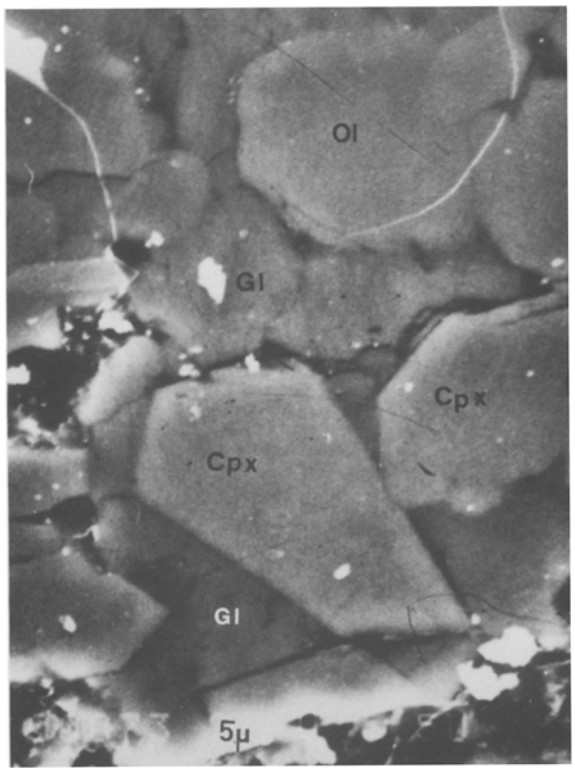

a

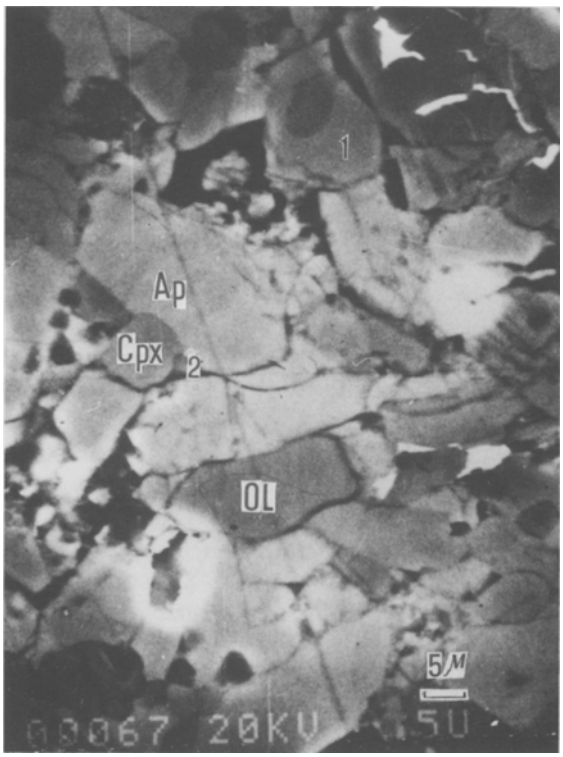

b

Fig. 1. Back-scattered electron images **a** Crystals of clinopyroxene (Cpx) and glass (Gl) in run products of experiment 2; **b** crystalline aggregate of apatite *Ap*, olivine *Ol* and clinopyroxene *Cpx* coexisting with the separated mass of glass in run products of experiment 3; grain 1 is clinopyroxene crystal with the core of orthopyroxene; 2—a thin film of glass may be seen between grains of clinopyroxene and apatite

Table 3. *Chemical compositions (mass.%) of starting mixtures and phases analyzed by electron microprobe in run products at 950 °C, 20 kbar*

Oxide		Starting mixture*	Glass		Apatite		Clinopyroxene		Olivine	
			Range	Mean	Range	Mean	Range	Mean	Range	Mean
			Phases in run products							
					Exp. 2					
1	SiO_2	23.67	0.7–03	0.4(4)**	0.07	0.07	53.62–51.51	52.69(11)	42.48–39.65	41.48
2	Al_2O_3	1.65	0.6–0.1	0.2(4)	—	—	7.39–5.91	6.89(11)	—	—
3	TiO_2	0.11	0.2	0.2(4)	0.03	0.03	1.15–0.46	0.81(11)	—	—
4	FeO	4.70	4.3–2.9	3.5(4)	0.16–0.16	0.16(2)	3.08–2.07	2.60(11)	9.52–8.25	8.65(6)
5	MgO	21.90	21.4–19.1	20.6(4)	0.30–0.28	0.29(2)	17.97–15.81	17.16(11)	48.75–52.12	50.23(6)
6	CaO	21.90	18.4–16.3	17.3(4)	52.71–50.49	51.60(2)	20.28–19.37	19.62(11)	0.22–0.40	0.31(2)
7	Na_2O	2.63	13.6–10.3	12.0(4)	0.07	0.07	2.31–1.73	1.95(11)	0.03–0.07	0.05(2)
8	Ce_2O_3	0.24	0.1–0.2	0.2(4)	0.57–0.49	0.53(2)	0.08–0.02	0.05(5)	0.04–0.1	0.03(2)
9	Yb_2O_3	—	—	—	—	—	—	—	—	—
10	P_2O_5	10.17	22.8–15.1	18.3(4)	41.95–40.62	41.28(2)	0.14–0.11	0.12(4)	0.05–0.01	0.07(2)
	Total	86.86		72.70		94.00		101.89		100.52
					Exp. 3					
1	SiO_2	24.06	11.36–7.02	9.88(4)	2.62–1.90	2.25(8)	51.64–49.52	50.87(3)	41.61–40.03	40.71(5)
2	Al_2O_3	1.80	3.84–2.26	2.74(4)	—	—	7.05–4.69	5.73(3)	n.d.	—
3	TiO_2	0.11	0.32–0.24	0.29(4)	—	—	0.55–0.49	0.52(2)	0.03–0.02	0.02(2)
4	FeO	4.78	1.93–1.62	1.73(4)	0.25–0.13	0.20(8)	1.69–1.29	1.49(2)	7.56–5.88	6.54(5)
5	MgO	22.03	12.48–10.98	11.69(4)	1.24–0.89	1.03(8)	16.00–17.26	16.48(3)	53.01–50.04	51.12(4)
6	CaO	20.28	29.96–25.06	28.00(4)	46.41–47.81	47.15(8)	21.80–23.20	22.60(3)	0.46–0.27	0.37(2)
7	Na_2O	2.5	10.39–4.38	7.09(4)	1.67–1.89	1.82(8)	0.99–0.82	0.93(3)	0.06–0.03	0.04(2)
8	Ce_2O_3	1.1	4.80–3.29	4.30(4)	5.94–4.98	5.42(8)	0.48–0.28	0.38(2)	0.13–0.09	0.11(2)
9	Yb_2O_3	0.9	2.61–1.82	2.26(4)	2.97–2.11	2.60(8)	0.89–0.70	0.79(2)	0.08–0.02	0.05(2)
10	P_2O_5	9.55	13.08–12.08	12.49(4)	34.65–35.44	35.11(7)	0.06–0.06	0.06(2)	0.06	0.06(2)
	Total	87.11	—	80.47	—	95.58	—	99.79	—	98.96

(Continued on page 8)

Table 3. (*cont.*)

	Oxide	Starting mixture*	Glass		Apatite		Clinopyroxene		Olivine	
			Range	Mean	Range	Mean	Range	Mean	Range	Mean
			Phases in run products							
					Exp. 4					
1	SiO_2	23.78	15.08–14.66	14.87(5)	2.41–2.41	2.41(2)	53.93–50.85	52.04(3)	41.90–41.60	41.72(3)
2	Al_2O_3	1.69	2.37–2.11	2.17(6)	—	—	4.02–3.24	3.75(3)	0.05–0.04	0.04(2)
3	TiO_2	0.11	0.43–0.36	0.40(6)	—	—	0.63–0.46	0.54(3)	0.05	0.05(1)
4	FeO	4.66	1.93–1.79	1.87(6)	0.21–0.11	0.16(2)	1.94–1.58	1.81(4)	5.57–4.48	5.08(4)
5	MgO	21.78	12.76–11.62	12.51(6)	1.00–0.98	0.99(2)	18.22–17.12	17.61(3)	52.74–51.29	52.77(4)
6	CaO	20.49	28.06–27.42	27.68(5)	48.39–48.48	48.44(2)	22.85–21.53	22.15(4)	0.50–0.45	0.50(2)
7	Na_2O	2.57	7.07–6.62	6.75(5)	1.16–1.11	1.14(2)	0.90–0.67	0.81(4)	0.05–0.03	0.04(2)
8	Ce_2O_3	1.4	3.43–3.12	3.23(6)	5.64–5.48	5.56(2)	0.58–0.45	0.52(3)	0.07	0.07(1)
9	Yb_2O_3	0.9	1.40–1.07	1.24(6)	1.51–1.46	1.48(2)	0.63–0.49	0.56(2)	0.07	0.07(1)
10	P_2O_5	9.62	14.74–14.10	14.37(5)	39.44–39.96	39.70(2)	0.31–0.15	0.23(2)	n.d.	—
	Total	87.00	—	85.09	—	99.88	—	100.02	—	100.34

* in exp. 2 mixture contains 0.08 Cr_2O_3, 0.12 MnO; 0.07 NiO; 12.68 CO_2 (of carbonates); in exp. 3—0.09 Cr_2O_3; 0.15 MnO; 0.07 NiO; 0.4 H_2O (of hydroxilapatite); 12.13 CO_2 (of carbonates); in exp. 4—0.11 Cr_2O_3, 0.15 MnO; 0.07 NiO; 0.41 H_2O (of hydroxilapatite); 12.26 CO_2 (of carbonates).

** Numbers in parentheses represent numbers of analysed points.

Table 4. *Partition coefficients (K) for interphase distribution of* Ce_2O_3 *and* Yb_2O_3 *from experimental results of the present work*

	Ce_2O_3			Yb_2O_3		
	Exp 2	Exp 3	Exp 4	Exp 2	Exp 3	Exp 4
Ap/Ol	17.7	49.3	79.4	—	52	21
Ap/Cpx	10.6	14.3	10.7	—	3.29	2.64
Ap/melt	2.6	1.3	1.7	—	1.13	1.23
Cpx/Ol	1.7	3.5	7.4	—	15.80	8.0
Ol/melt	0.15	0.02	0.06	—	0.02	0.06
Cpx/melt	0.25	0.09	0.16	—	0.34	0.46

coefficients. Thus it is suggested that our data, which is the first available for REE behaviour during the partial melting of carbonatised apatite-bearing peridotite at mantle pressure, can be used with confidence in modelling mantle melting processes.

The carbonate-phosphate melts encountered in this project must have a very different structure to the more usual silicate partial melts, and it is not surprising therefore that K_D-values are significantly different. For example, our $K_D = (Mg/Fe)^{liq}/(Mg/Fe)^{solid}$ for both clinopyroxene and olivine are all more than 0.5, and in run 2, in which the silica content of the melt was the lowest encountered, this value is close to 1. These values may be compared to $\simeq 0.3$ for olivine in olivine in komatiite and basaltic melt and $\simeq 0.2$ for clinopyroxene (*Takahashi* and *Kushiro*, 1983). This much weaker fractionation of Fe into the liquid phase and Mg into the crystal phase during fractional crystallisation may have a profound effect on composition trends, e.g. the early formed silicate crystals will be somewhat poorer in Mg compared to say a basaltic system, but this moderately high Mg content would persist over a large temperature interval. These deductions might explain the common occurence of minerals with high Mg-numbers in some rock members found in carbonatite complexes.

Our experimental data demonstrate that Na contents in carbonate-phosphate melts equilibrated with multicomponent peridotite mineral assemblages including jadeite-bearing clinopyroxene are quite high. Similar results were obtained in previous studies on the melting of apatite-bearing and phosphorus-free carbonatised peridotites (*Wallace* and *Green*, 1988; *Ryabchikov* et al., 1991, 1993). Figure 2 shows the pressure dependence of Na partition coefficients between clinopyroxene and carbonatitic melt deduced from both our experimental data and the results of previously published works. It can be seen that, notwithstanding the presence or absence of excess P_2O_5 in the system experimental points plot near the common smooth curve. An increase in pressure results in a distinct drop in the alkali content of the carbonatitic melt.

The presence of high Na_2CO_3 concentrations in carbonate-phosphate liquids, equilibrated with mantle material, shifts the solidus to quite low temperatures. Conditions in our experiments (950 °C and 20 kbar) are very close to geothermobarometric estimates for many spinel-garnet lherzolite nodules from alkali basaltic volcanoes, e.g., mantle xenoliths from effusives of Shavaryn-Tsaram volcano (Mongolia) yield pressures between 17 and 20 kilobars and temperatures between 1000 and 1100° (*Ryabchikov* et al., 1983). Under these conditions any oxidized carbon and probably also P_2O_5 in the mantle rocks would be present as intergranular films of melt. It has been shown in the present work, that this mobile phase should intensely extract REE's from the host rock.

The upward migration of carbonate-phosphate melt may result in the creation, within the upper mantle, of zones enriched in REE, P_2O_5 and other incompatible components. The

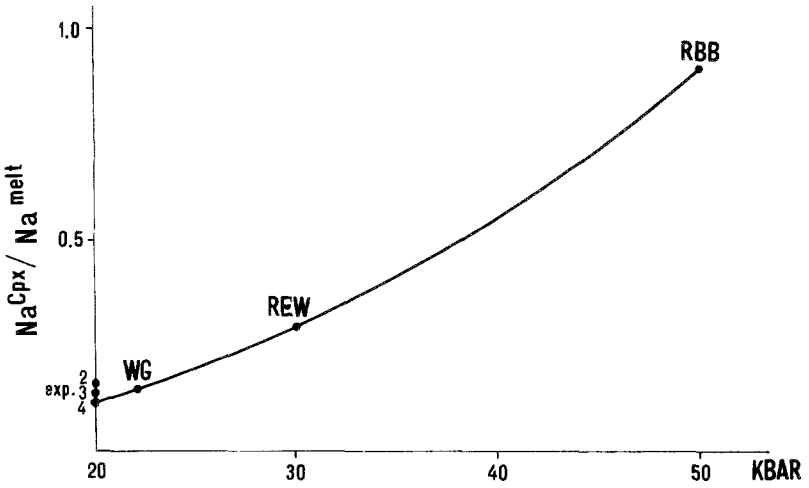

Fig. 2. Partition coefficient of Na beteeen clinopyroxene and carbonatitic liquid as a function of pressure. Exp. 2, 3, 4 are experimental points from the present work; *WG Wallace* and *Green*, 1988; *REW Ryabchikov* et al., 1991; *RBB Ryabchikov* et al., 1993)

solidification of the carbonatitic magmas may be caused by cooling, drop in pressure and migration of melt into the rocks with a lower chemical potential of sodium. In the last case the decrease of Na_2CO_3 concentration in the liquid phase should take place leading to the increase in solidus temperature. The action of such mechanism is corroborated by the commonly observed relative enrichment in light REE and other incompatible components of refractory mantle peridotites improverished in sodium, calcium and other typical "basaltic" components as compared to primitive lherzolites (*Nickel* and *Green*, 1984; *Stosch* and *Seck*, 1980). Thus, these low-Na and low-Ca rocks, which previously underwent large-scale partial melting, represent geochemical barriers for many rare elements. When carbonatitic liquids ascend in the mantle, their degassing should take place at a certain level, which should result in the complete crystallisation of the melt. It may be recalled that the presence in mantle olivines of fluid microinclusions filled by dense CO_2 is usually accompanied by elevated REE contents which are likely to be present in the form of tiny crystalline inclusions.

The presence in some mantle rocks of intergranular finely crystalline films precipitated from carbonate-phosphate melts is corroborated by experiments on the acid treatment of mantle minerals. The leached material is as a rule enriched in incompatible elements compared with bulk samples, and is often characterized by isotopic ratios distinct from bulk samples. Migration of REE's in the form of carbonate-phosphate melts is consistent with proven positive correlation of these elements with P_2O_5 in mantle rocke and magmas of mantle genesis (*Jochum* et al., 1986).

Conclusions

1) Carbonate-phosphate liquids equilibrated with mantle peridotites at 20 kbar and 950 °C may be quenched into homogeneous low-silica glasses.

2) The P_2O_5 contents of these carbonate- phosphate- melts equilibrated with apatite-bearing wehrlite at these P and T are approximately 18 wt%.

3) REE's are intensely extracted by carbonate-phosphate melts from silicate mantle minerals. The measured partition coefficients for apatite + carbonatitic melt

pairs are similar to previously published data for the equilibrium of apatite with basanitic melt (*Watson* and *Green*, 1981).

4) The difference of Mg/Fe ratios in carbonate-phosphate liquids and coexisting ferromagnesian silicate crystals is significantly smaller than in the case of silicate magmas. This should result in the slower increase in Fe/Mg ratios during fractional crystallisation of carbonatitic melts.

5) The extraction of Na_2O from clinopyroxenes by carbonatitic melts is significantly more intense at 20 kbar compared with higher pressures (*Ryabchikov* et al., 1991, 1993).

6) High Na_2CO_3 contents in carbonatitic melts equilibrated with natural peridotites noticeably depress solidus temperatures, which thus become similar to the geothermobarometric estimates for garnet-spinel lherzolitic nodules from alkali basaltic rocks. Under these conditions, carbonate-phosphate intergranular melts may represent, the common form for oxidized carbon and phosphorus in mantle material.

7) The migration of such melts may represent one of the principal mechanisms for the redistribution of P_2O_5 and REE's within the upper mantle.

Acknowledgements

The authors are grateful to Dr. *D. L. Hamilton* and two anonymous Mineralogy and Petrology reviewers whose advice and criticism has greatly improved this paper.

References

Agaphonov LV, Erkushov YuA (1988) Distribution coefficients of REE and model calculations of the partial melting and fractional crystallisation. In: Rare earth elements in magmatic rocks. Acad. Sci. USSR, Sib. Div., Institute of Geol. Geoph., Novosibirsk, 101–124 (in Russian)

Bailey DK (1989) Carbonatite melt from the mantle in the volcanoes of south-east Zambia. Nature 338: 415–418

Baker MB, Wyllie PJ (1990a) Liquid immiscibility in a nephelinite-carbonate system at 25 kbar and implications for carbonatite origin. Nature 346: 168–170

Baker MB, Wyllie PJ (1990b) High-pressure solubility of apatite in carbonate-rich melts (abstr). Eos 71: 648

Brennan JM, Watson EB (1991) Partitioning of trace elements between carbonate melt and clinopyroxene and olivine at mantle P-T conditions. Geochim Cosmochim Acta 55: 2203–2214

Green DH, Wallace ME (1988) Mantle metasomatism by ephermeral carbonatite melts. Nature 336: 459–462

Green TH, Sie SH, Ryan CG, Cousens DR (1989) Proton microprobe determined partitioning of Nb, Ta, Zr, Sr, and Y between garnet, clinopyroxene and basaltic magma at high pressure and temperature. Chem Geol 74: 201–214

Hornig I, Keller J (1990) Rare earth elements in carbonatites and their mineral phases. Abstracts Int Volcanological Congr Mainz.

Hunter RH, McKenzie D (1989) The equilibrium geometry of carbonate melts in rocks of mantle composition. Earth Planet Sci Lett 92: 347–356

Irving AJ, Frey FA (1984) Trace element abundances in megacrysts and their host basalts: constraints on partition coefficients and megacryst genesis. Geochim Cosmochim Acta 48: 1201–1221

Jochum KP, Hofmann AW, Seufert HM (1986) Uniform ratios of incompatible trace elements in oceanic basalts. Terra Cognita 6: 186

Jones KP, Wyllie PJ (1983) Low-temperature glass quenched from a synthetic rare earth cabonatite: implication for the origin of the Mountain Pass deposit, California. Econ Geol 78: 1721–1723

Mysen BO (1978) Experimental determination of rare earth element partitioning between hydrous silicate melt, amphibole and garnet peridotite minerals at upper mantle pressures and temperatures. Geochim Cosmochim Acta 42: 1253–1263

Nickel KG, Green DH (1984) The nature of the upper-most mantle beneath Victoria, Australia, as deduced from ultramafic xenoliths. Proceed 3rd Int Kimberlite Conf 2: 330–338

Ryabchikov D, Brey GP, Bulatov VK (1993) Carbonate melts Coexisting with mantle peridotites at 50 kbar. Petrology 1 (2): 159–163

Ryabchikov ID, Edgar AD, Wyllie PJ (1991) Partial melting in the system carbonate-phosphate-peridotite at 30 kbar. Geokhimiya N 2: 163–168 (in Russian)

Ryabchikov ID, Kovalenko VI, Ionov DA, Solovova IP (1983) Thermodynamic parameters of mineral equilibria in garnet-spinel lherzolites of Mongolia. Geokhimiya N 7: 967–980 (in Russian)

Ryabchikov ID, Orlova GP, Kalenchuk GE (1989) The interaction of spinel lherzolite with water-carbon dioxide fluid at 20 kbar and 900 °C. Geokhimiya N 3: 385–392

Stosch HG, Seck HA (1980) Geochemistry and mineralogy of two spinel peridotite suites from Dreiser Weiher, West Germany. Geochim Cosmochim Acta 44: 457–470

Takahashi E, Kushiro I (1983) Melting of dry peridotite at high pressures and basalt magma genesis. Am Mineral 44 (2): 859–879

Wallace ME, Green DH (1988) An experimental determination of primary carbonatite magma compositions. Nature 335: N 6188: 343–346

Wass SY, Henderson P, Ellitt CJ (1980) Chemical heterogenity and metasomatism in the upper mantle: evidence from rare earth and other elements in apatite-rich xenoliths in basaltic rocks from Eastern Australia. Phil Trans Roy Soc Lond 297: 333–346

Watson EB, Green TH (1981) Apatite liquid partition coefficients for the rare earth elements and strontium. Earth Planet Sci Lett 56: 405–421

Wendlandt RF, Harrison WY (1979) Rare earth partioning between carbonate and silicate liquids and CO_2 vapor: results and implications for the formation of light rare earth-enriched rocks. Contrib Mineral Petrol 69: 409–419

Wyllie PJ, Baker MB, White BS (1990) Experimental boundaries for the origin and evolution of carbonatites. Lithos 26: 3–19

Zindler A, Jagoutz E (1988) Mantle cryptology. Geochim Cosmochim Acta 52: 319–333

Authors' address: Dr. *I. D. Ryabchikov*, Institute for Geology of Ore Deposits, Petrography, Mineralogy and Geochemistry Academy of Sciences, Moscow, Russia